Acta Crystallographica Section D
Biological Crystallography
ISSN 0907-4449

Structure of the lipopeptide antibiotic tsushimycin

Gábor Bunkóczi,[a]*‡ László Vértesy[b] and George M. Sheldrick[a]

[a]Lehrstuhl für Strukturchemie, Georg-August Universität, Tammannstrasse 4, 37077 Göttingen, Germany, and [b]Aventis Pharma Deutschland GmbH, Division LG Natural Products, 65926 Frankfurt am Main, Germany

‡ Current address: Structural Genomics Consortium, University of Oxford, Botnar Research Centre, Oxford OX3 7LD, England.

Correspondence e-mail: gabor.bunkoczi@sgc.ox.ac.uk

Received 11 April 2005
Accepted 31 May 3005

PDB Reference: tsushimycin, 1w3m, r1w3msf.

The amphomycin derivative tsushimycin has been crystallized and its structure determined at 1.0 Å resolution. The asymmetric unit contains 12 molecules and with 1300 independent atoms this structure is one of the largest solved using *ab initio* direct methods. The antibiotic is comprised of a cyclodecapeptide core, an exocyclic amino acid and a fatty-acid residue. Its backbone adopts a saddle-like conformation that is stabilized by a Ca^{2+} ion bound within the peptide ring and accounts for the Ca^{2+}-dependence of this antibiotic class. Additional Ca^{2+} ions link the antibiotic molecules to dimers that enclose an empty space resembling a binding cleft. The dimers possess a large hydrophobic surface capable of interacting with the bacterial cell membrane. The antibiotic daptomycin may exhibit a similar conformation, as the amino-acid sequence is conserved at positions involved in Ca^{2+} binding.

1. Introduction

Lipopeptide antibiotics constitute a class of antibacterial agents that are highly active against multi-resistant bacteria. Amphomycin, the first member of the series, was discovered more than 50 years ago (Heinemann *et al.*, 1953) and was followed by the isolation of tsushimycin (Shoji *et al.*, 1968) and other antibiotics belonging to the same group. Amphomycins possess a peptide framework consisting of a ten-member cyclopeptide ring and an exocyclic amino acid, the α-NH_2 group of which is acylated by a fatty-acid residue (Fig. 1).

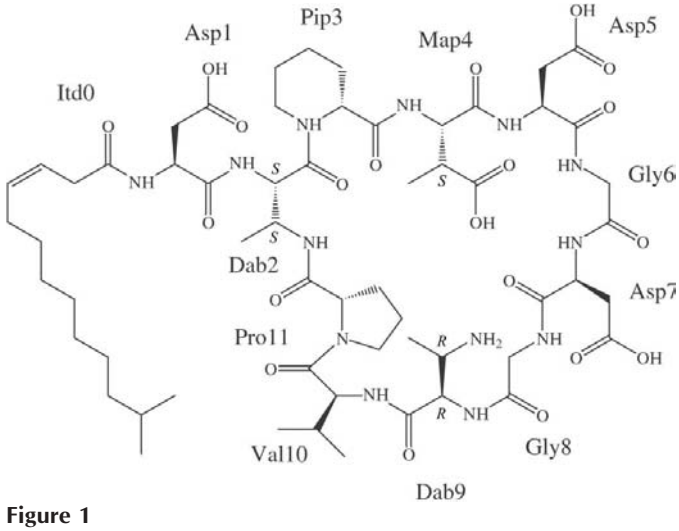

Figure 1
Chemical structure of tsushimycin. Amphomycin differs by having a slightly modified fatty-acid residue, while friulimicin B has Asn1 instead of Asp1. Itd, Δ3-isotetradecenoic acid; Dab, 2,3-diaminobutyric acid; Pip, pipecolinic acid; Map, β-methylaspartate.

Antibiotics in this series differ principally in the structure of the fatty-acid substituent. Daptomycin, a recently approved last-resort antibiotic, may also belong to this group as indicated by the ten-membered cyclopeptide core and the fatty-acid constituent, although the amino-acid sequence is markedly different (Debono *et al.*, 1988).

Amphomycin was found to be active against Gram-positive bacteria, but its exact mechanism of action has not been conclusively determined. Early studies indicated amphomycin to be a specific inhibitor of bacterial cell-wall synthesis, acting at the level of phospho-*N*-acetylmuramoyl-pentapeptide-transferase (MraY), which catalyses the transfer of the UDP-MurNAc-pentapeptide to the undecaprenyl carrier (Tanaka *et al.*, 1982). On the other hand, there is still an ongoing debate on the mode of action of daptomycin. It was first reported to act by inhibiting peptidoglycan biosynthesis at the stage of the formation of the nucleotide-linked sugar–peptide precursors (Allen *et al.*, 1987). However, it was later found that daptomycin did not enter the cell and the synthesis of lipoteichoic acids occurring in the cytoplasmic membrane was proposed as the site of action (Canepari *et al.*, 1990), which has recently been disproved (Laganas *et al.*, 2003). The dissipation of membrane potential upon the action of daptomycin (Alborn *et al.*, 1991) and a correlation with bactericidal activity (Silverman *et al.*, 2003) has also been noted, but recent evidence suggests that membrane depolarization is more likely to be the consequence than the cause of antimicrobial action (Jung *et al.*, 2004).

Lipopeptide antibiotics possess superior antibacterial potency. They are rapidly bactericidal against, for example, multi-resistant *Staphylococcus aureus* and most enterococci. Resistance to lipopeptide antibiotics is rare; daptomycin, the only member being evaluated in clinical trials, is active against 99% of tested clinical isolates (Barry *et al.*, 2001). The level of Ca^{2+} ions in the medium proved to be important in tests against less susceptible isolates; in trials on Ca^{2+}-supplemented media corresponding to physiological Ca^{2+} levels, minimum inhibitory concentration values were found to be twofold to fourfold lower. Given their superior antibacterial activity, primarily against problematic microbes, lipopeptides are perfect antibiotics for reinforcing or replacing glycopeptides as a last line of defence against deadly bacterial infections.

2. Materials and methods

2.1. Crystallization and data collection

The isolation and purification of tsushimycin has already been described (Vértesy *et al.*, 2000). Aliquots of a 40 mg ml^{-1} tsushimycin solution were mixed with equal volumes of a reservoir solution containing 0.1 *M* sodium acetate/acetic acid pH 4.0, 0.12 *M* acetic acid, 38% ethanol, 0.40 *M* 1,6-hexanediol and 0.80 *M* $CaCl_2$ and crystallized at room temperature using the hanging-drop method. Thin plate crystals with maximum dimensions up to 0.5 × 0.5 × 0.05 mm were obtained over a period of several weeks. For measurement, a suitable crystal was taken out with a loop, mounted in a cold nitrogen stream and data sets were collected at the BL1 beamline at BESSY at 0.90 Å wavelength using a MAR CCD detector. Diffraction maxima could be observed to 1.0 Å resolution; owing to anisotropic reflection profiles the data sets were collected using relatively thin slicing (0.5°) and processed using *XDS* (Kabsch, 2001). As crystals belong to space group *P*1 (unit-cell parameters a = 33.49, b = 36.39, c = 37.52 Å, α = 65.6, β = 68.4, γ = 69.9°), several passes were necessary reorienting the crystal (using a goniometer head with adjustable rotation axes) after each pass to achieve acceptable completeness. A total of 355 145 reflections were measured, of which 75 901 were unique with the following data statistics (overall/1.10–1.00 Å): completeness 96.2/92.1%, redundancy 4.50/3.63, $\langle I/\sigma\langle I\rangle$ 9.49/3.35, $R_{\rm int}$ ($= \sum I - \langle I\rangle/\sum I$) 0.1039/0.4990.

2.2. Structure solution and refinement

Probably owing to the distribution of Ca^{2+} ions in the unit cell and the superior resolution, the structure could be easily solved *via ab initio* direct methods using the program *SHELXD* (Sheldrick *et al.*, 2001). The Ca^{2+} ions were first located using dual-space recycling and then peak-list optimization was performed in ten steps to expand the structure from 30 atoms to 1300. The unexpectedly high success rate (nearly each try corresponded to the right solution) provoked a more detailed analysis and *SHELXD* was rerun with different high-resolution cutoffs. It was found that a solution could be obtained even with data truncated to 1.5 Å which, when using *SHELXE* (Sheldrick, 2002) for density modification with the

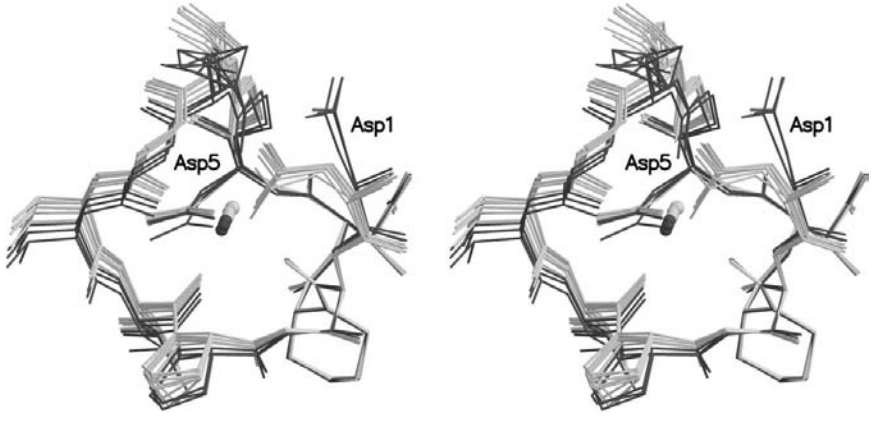

Figure 2
Stereoview of the superposition of all 12 independent antibiotic molecules. Rigid fragments (corresponding to residues Dab2–Map4) were identified with *ESCET* (Schneider, 2002) and fitted using *LSQKAB* (Kabsch, 1976). Although the rigid part comprises only three out of 11 residues, the overall conformation is fairly similar and the only deviation seems to be the side-chain conformation of Asp1, which either takes part in coordinating the central Ca^{2+} ion (light-coloured molecules) or does not (dark-coloured molecules). The Ca^{2+} ions are coloured according to the antibiotic molecule they associate with. The figure was created using *MOLSCRIPT* (Kraulis, 1991) and *RASTER3D* (Merritt & Bacon, 1997).

full 1.0 Å data set, resulted in the same high-quality electron-density map (MapCC, the map correlation coefficient relative to final refined model, was 0.896). For the solution obtained at 1.5 Å, density modification was also performed using data extending to the same resolution. Despite the relatively high MapCC obtained (0.733), the final map would be difficult to trace because of the presence of a high proportion of non-conventional amino acids and the resulting non-standard structure.

With 1300 independent atoms, tsushimycin occupies a prominent place in the list of structures solved by *ab initio* direct methods (Sheldrick *et al.*, 2001); it is also noteworthy that in the case of the largest *ab initio* solved structure, cytochrome c_3, the heaviest atom was Fe, which is heavier than Ca and therefore facilitates the solution (Frazão *et al.*, 1999). On the other hand, the largest equal-atom structure (containing no atom heavier than oxygen), structures which are much more resistant to solution by direct methods than those containing a number of heavier atoms, is also over 1000 atoms (Bunkóczi *et al.*, 2005).

The model was built atom by atom using *XtalView* (McRee, 1999) from an electron-density map generated by *SHELXE*; 11 896 parameters corresponding to 1260 non-H atoms were refined against all unique reflections in the resolution range 26.0–1.0 Å using *SHELXL* (Sheldrick & Schneider, 1997). Throughout the refinement, bond length, bond angle, chiral volume and planarity restraints were imposed on appropriate atoms. Solvent atoms were added using *SHELXWAT* and manually. All non-H atoms were refined anisotropically using suitable rigid-bond and similarity restraints. For solvent waters, approximately isotropic restraints were also employed. H atoms were included in the later stages of refinement. About 5% of the reflections (selected in thin shells) were reserved for the calculation of $R_{\rm free}$. The refinement converged to a crystallographic R factor of 0.123/0.137 ($F > 4\sigma$/all data) and an $R_{\rm free}$ of 0.156/0.171.

3. Results

3.1. Peptide conformation

12 independent antibiotic molecules are present in the asymmetric unit, each of which binds a Ca^{2+} ion. Peptide atoms are well defined in the electron density, while most of the fatty-acid side chains are continuously disordered. There are large cavities in the unit cell that are filled with water or disordered alkyl chains. The molecules exhibit nearly identical conformation, as indicated by the mean-square deviation between the main-chain atoms after least-squares fitting, which varies in the range 0.1–0.5 Å (Fig. 2). The shape of the peptide backbone resembles a saddle with a long tail; the Ca^{2+} ion is bound in the middle of the saddle (Fig. 3*a*).

3.2. Calcium binding

Four backbone carbonyl O atoms, two side-chain carboxyl groups from aspartate residues and a water molecule coordinate the Ca^{2+} ion in a slightly distorted pentagonal bipyramidal arrangement (Fig. 3*b*). Calcium–oxygen distances vary in the range 2.3–2.5 Å, with the water molecule being the most distant and the axial carboxyl O atoms closest. This may suggest that the aspartate side chains are deprotonated and negatively charged at the pH of crystallization. It is interesting to note that the aspartate residues taking part in Ca^{2+} binding (Asp1 and Asp5) are also conserved in daptomycin (Asp3 and Asp7) and despite the markedly different amino-acid sequence, the Ca^{2+} binding and probably the structure of the cyclopeptide core may be analogous. For three of the 12 molecules in the asymmetric unit, the side chain of Asp1 in the

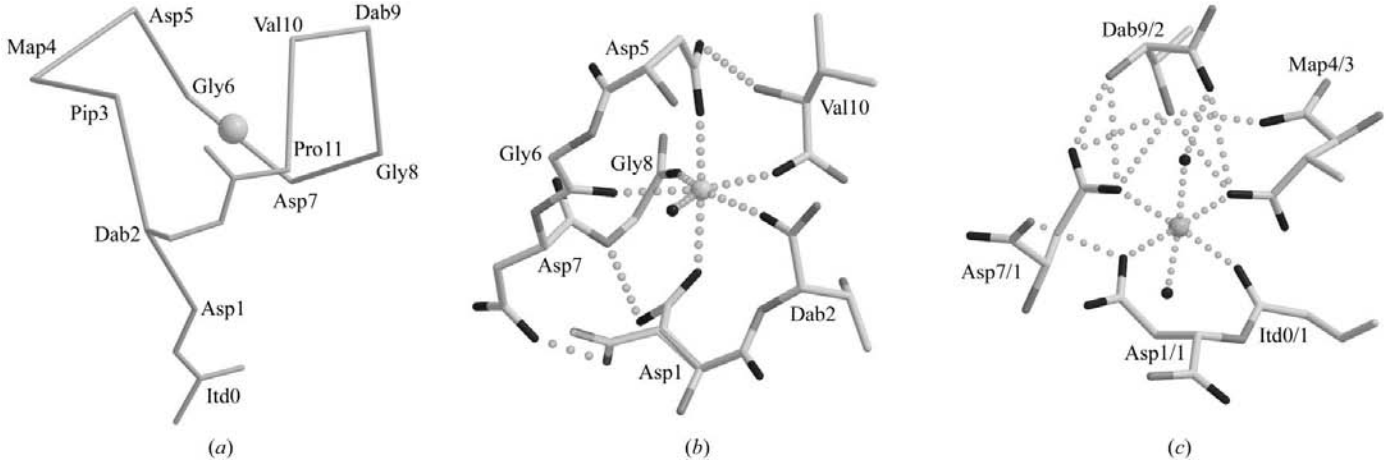

Figure 3
(*a*) Backbone trace for tsushimycin. The isotetradecenoyl side chain has been truncated for clarity. (*b*) The central Ca^{2+} ion is surrounded by seven atoms with pentagonal bipyramidal geometry. Hydrogen bonds fixing the side chains of Asp1 and Asp5 are also shown. The alternative open conformation for Asp1 (present in 25% of the independent molecules) is displayed transparently. (*c*) The octahedral coordination of the peripheral Ca^{2+} ion. The amino acids belong to three different antibiotic molecules (indicated by the number after the solidus). Molecules 1 and 2 form a dimer. In the minor conformation, the side chain of Asp1/1 occupies an axial position and displaces the bottom water molecule (not shown). These figures were drawn using *MOLSCRIPT*/*RASTER3D*.

coordination sphere of the Ca^{2+} ion was found to be displaced by a water molecule (Fig. 2); this arrangement may provide a mechanism for the process of entry of the Ca^{2+} ion into the central cavity of the antibiotic.

Apart from the intramolecular interactions involved in coordinating the Ca^{2+} ion, only a few stabilizing hydrogen bonds can be identified. Most of these hold the side chains of Asp1 and Asp5 in the appropriate position for Ca^{2+} coordination or the side chain of Asp1 in the alternative open conformation. These interactions are likely to be too weak to provide the antibiotic with the rigidity observed in the crystal structure (judged from the comparison of the different molecules), so the central Ca^{2+} ion probably plays a decisive role in determining the conformation of the molecule. It is plausible that the antibiotic has no well defined conformation in the absence of Ca^{2+} and consequently cannot exert its inhibitory effect, which could account for the observed Ca^{2+}-dependence of this antibiotic group.

On the molecular surface, each molecule binds an additional Ca^{2+} ion, which is surrounded by a main-chain carbonyl O atom, three carboxyl groups and two water molecules completing a regular octahedron (Fig. 3*c*). Although it may also contribute to the stability of the three-dimensional structure, it is more likely that this ion acts as a linker between individual antibiotic molecules.

3.3. Association

The antibiotic molecules form dimers, which are connected by hydrogen bonds and interactions mediated by the peripheral Ca^{2+} ions. The dimerization results in a structure with the hydrophobic groups concentrated on one side of the dimer, while the flat surface that is formed on the opposite side is markedly hydrophilic. The dimers are linked by hydrogen bonds between Asp7 of the first molecule and Dab9 from the second and *vice versa*. Additionally, Asp7 is involved in binding the peripheral Ca^{2+} ion, which is also linked to Dab9 of the second antibiotic *via* a water molecule.

The two molecules in a dimer enclose empty space that is open at both two ends and constitutes a tunnel. The peripheral Ca^{2+} ions are located near the two ends of the tunnel, which has an additional opening at the middle (Fig. 4). The tunnel surface is highly charged near the Ca^{2+} ions at the entrance and weakly hydrophilic in between.

The dimers are interconnected by a salt bridge between the peripheral Ca^{2+} ion and the carboxyl group of Map4. The two Map4 residues in a dimer occupy the two extreme positions on the flat hydrophilic surface and at the same time the most distant positions from the dimer interface (Fig. 4). Each dimer is connected to two other dimers and the whole asymmetric unit is thus cross-linked. The dimers are arranged in such a way that their hydrophobic sides with the fatty-acid side chains surround a cavity, while the charged groups of the molecules point outside and constitute a polar surface. This arrangement corresponds to the structure of a micelle, which is slightly elongated in one dimension.

3.4. Comparison with related structures

The solution structure of daptomycin has recently been reported by two independent groups [apo-daptomycin, PDB code 1t5m; Ca^{2+}-daptomycin, PDB code 1t5n (Jung *et al.*, 2004); apo-daptomycin, PDB code 1xt7 (Ball *et al.*, 2004)]. Although these structures are not directly comparable to tsushimycin in view of not only the different chemical species but also the subtle changes the molecule may undergo upon Ca^{2+} binding, the models were superimposed and the result visually evaluated. Although the conformation of some NMR models is reminiscent of that of tsushimycin, none of the daptomycin NMR structures is sufficiently similar to allow a direct comparison. The residual mean-square deviation (r.m.s.d.) between the main-chain atoms after least-squares fitting varies between 2.2 and 3.2 Å. Moreover, in terms of r.m.s.d. the tsushimycin backbone proved to be less similar to the Ca^{2+}-daptomycin structure than to any of the apo-daptomycin models. It should also be noted that the similarity between the apo-daptomycin NMR models determined by the two independent groups is also not satisfactory (r.m.s.d. ranges 2–3 Å). Neither in the Ca^{2+}-daptomycin structure nor in the apo-daptomycin models can a Ca^{2+}-binding arrangement of O atoms analogous to that seen in tsushimycin be detected.

4. Discussion

Based on the crystal structure, the biologically active species of tsushimycin is most likely to be the dimer. Since dimers are associated so that they expose highly polar surfaces to the solvent, it is unlikely that they penetrate the bacterial cell membrane, but they can interact with it by means of their fatty-acid side chain. The enclosed free space between the two monomers is large enough to accommodate a substrate, which

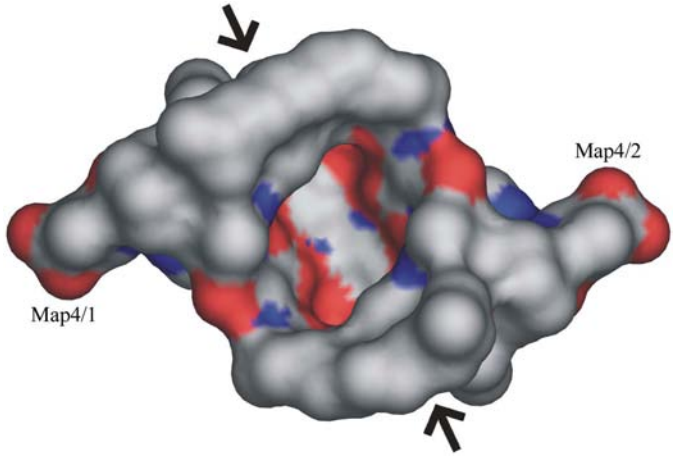

Figure 4
Top surface view of a tsushimycin dimer. The figure is colour-coded according to charge: red, negative; blue, positive. The interdimer tunnel runs in the plane (the entrances are marked by arrows) and the central opening is shown at the middle. The Map4 residues interconnecting dimers are linked to peripheral Ca^{2+} ions, which are at the tunnel entrances. This figure was drawn using *PyMol* (DeLano Scientific; http://www.pymol.org).

can either be neutral or anionic, in the latter case most likely interacting with one of the bound Ca^{2+} ions.

Despite the large deviations established when comparing tsushimycin with daptomycin NMR models, it is likely that daptomycin assumes a similar conformation and binds Ca^{2+} ions specifically and in a similar manner to tsushimycin, since despite the low sequence homology all amino acids involved in Ca^{2+} binding are conserved. On the other hand, the active species may be different from a dimer in the case of daptomycin, since the amino acid corresponding to Dab9 is replaced by a serine, although that corresponding to Asp7 is conserved. The amino acid primarily involved in connecting tsushimycin dimers (Map4) is substituted by an ornithine in the daptomycin sequence, which cannot bind a Ca^{2+} ion, but could link dimers in an analogous way by forming a salt bridge with one of the nearby aspartate residues. The small number of long-range distance constraints available from NMR may explain the dissimilarity of the NMR models and the tsushimycin X-ray structure. The possibility of intermolecular interactions such as those observed in the X-ray structure was not taken into account in the NMR analyses. In particular, secondary interactions that are involved in linking tsushimycin dimers (*e.g.* Asp7–Dab9) would give rise to NOEs between residues close in sequence but not in space and therefore could easily mislead the structure determination. Although the solution structure of tsushimycin may differ from that in a crystal, the presence of 12 independent molecules, each in a unique environment but in virtually the same conformation, rules out the possibility that 'crystal contacts' significantly affect the structure.

The tsushimycin structure strongly supports the hypothesis by Silverman *et al.* (2003) and its modification by Jung *et al.* (2004) for the mechanism of action of this antibiotic group. The dimers seen in the crystal may well be important in the proposed oligomerization step and linkage of tsushimycin dimers *via* the Ca^{2+} bridge may be the basis. A clear explanation for the means of interaction between the antibiotic and acidic phospholipids is also offered by the tsushimycin dimer: the polar part of a phospholipid molecule can be bound in the tsushimycin tunnel (Fig. 4) and the long aliphatic chains can exit through the hole, which points towards the membrane. It is likely that the fatty-acid side chains of the antibiotic also take part in the interaction, as both of them point in this direction.

We are grateful to the Fonds der Chemischen Industrie and the Deutsche Forschungsgemeinschaft (SFB416) for support and to the PSF/BESSY for the data-collection opportunity.

References

Alborn, W. E. Jr, Allen, N. E. & Preston, D. A. (1991). *Antimicrob. Agents Chemother.* **35**, 2282–2287.
Allen, N. E., Hobbs, J. N. Jr & Alborn, W. E. Jr (1987). *Antimicrob. Agents Chemother.* **31**, 1093–1099.
Ball, L.-J., Goult, C. M., Donarski, J. A., Micklefield, J. & Ramesh, V. (2004). *Org. Biomol. Chem.* **2**, 1872–1878.
Barry, A. L., Fuchs, P. C. & Brown, S. D. (2001). *Antimicrob. Agents Chemother.* **45**, 1919–1922.
Bunkóczi, G., Vértesy, L. & Sheldrick, G. M. (2005). *Angew. Chem. Intl. Ed.* **44**, 1340–1342.
Canepari, P., Boaretti, M., Lleó, M. M. & Satta, G. (1990). *Antimicrob. Agents Chemother.* **34**, 1220–1226.
Debono, M., Abbot, B. J., Molloy, R. M., Fukuda, D. S., Hunt, A. H., Daupert, V. M., Counter, F. T., Ott, J. L., Carrell, C. B., Howard, L. C., Boeck, L. D. & Hamill, R. L. (1988). *J. Antibiot.* **41**, 1093–1105.
Frazão, C., Sieker, L., Sheldrick, G., Lamzin, V., LeGall, J. & Carrondo, M. A. (1999). *J. Biol. Inorg. Chem.* **4**, 162–165.
Heinemann, B., Kaplan, M. A., Muir, R. D. & Hooper, I. R. (1953). *Antibiot. Chemother.* **3**, 1239–1242.
Jung, D., Rozek, A., Okon, M. & Hancock, R. E. W. (2004). *Chem. Biol.* **11**, 949–957.
Kabsch, W. (1976). *Acta Cryst.* A**32**, 922–923.
Kabsch, W. (2001). *International Tables for Crystallography*, Vol. *F*, edited by M. G. Rossmann & E. Arnold, pp. 218–225. Dordrecht: Kluwer Academic Publishers.
Kraulis, P. J. (1991). *J. Appl. Cryst.* **24**, 946–950.
Laganas, V., Alder, J. & Silverman, J. A. (2003). *Antimicrob. Agents Chemother.* **47**, 2682–2684.
McRee, D. E. (1999). *J. Struct. Biol.* **125**, 156–165.
Merritt, E. A. & Bacon, D. J. (1997). *Methods Enzymol.* **277**, 505–524.
Schneider, T. R. (2002). *Acta Cryst.* D**58**, 195–208.
Sheldrick, G. M. (2002). *Z. Kristallogr.* **217**, 644–650.
Sheldrick, G. M., Hauptmann, H. A., Weeks, C. M., Miller, R. & Usón, I. (2001). *International Tables for Crystallography*, Vol. *F*, edited by M. G. Rossmann & E. Arnold, pp. 333–351. Dordrecht: Kluwer Academic Publishers.
Sheldrick, G. M. & Schneider, T. R. (1997). *Methods Enzymol.* **277**, 319–343.
Shoji, J., Kozuki, S., Okamoto, S., Sakazaki, R. & Otsuka, H. (1968). *J. Antibiot.* **21**, 439–443.
Silverman, J. A., Perlmutter, N. G. & Shapiro, H. M. (2003). *Antimicrob. Agents Chemother.* **47**, 2538–2544.
Tanaka, H., Ōiwa, R., Matsukura, S., Inokoshi, J. & Ōmura, S. (1982). *J. Antibiot.* **35**, 1216–1221.
Vértesy, L., Ehlers, E., Kogler, H., Kurz, M., Meiwes, J., Seibert, G., Vogel, M. & Hammann, P. (2000). *J. Antibiot.* **53**, 816–827.